International Conference on Applied Energy
ICAE 2013, Jul 1-4, 2013, Pretoria, South Africa
Paper ID: ICAE2013-300

SATURATION TOWER DESIGN FOR MICRO HUMID AIR TURBINE APPLICATIONS

Ward De Paepe[1], Francesco Contino[1], Frank Delattin[1], Svend Bram[1,2], Jacques De Ruyck[1]

1 Vrije Universiteit Brussel, Dept. of Mechanical Engineering, Pleinlaan 2, 1050 Brussel, Belgium

2 Erasmushogeschool Brussel, Dept. of Industrial Sciences and Technology, Nijverheidskaai 170, 1070 Brussels, Belgium

ABSTRACT

The micro Humid Air Turbine (mHAT) has proven to have the highest potential of all mixed air/water micro Gas Turbines (mGTs). Turning a mGT into a mHAT however requires the installation of a saturation tower. Most common saturation towers use packing material to increase the contact area between compressed air and water. The packing material however causes a pressure drop, which has a severe negative effect on the mGT performance. To limit this pressure drop, we have developed a spray tower without packing that uses nozzles to inject water in the compressed air. In this paper, we propose a design for the spray tower based on two-phase flow simulations. The two major constraints during the design were minimal pressure loss and tower size. A sensitivity analysis was performed in order to indicate the key parameters to obtain fully saturated air from the tower. Results of simulations showed that using a spray tower reduces the pressure losses significantly when compared to a classic saturation tower. Sensitivity analysis showed that droplet diameter and injected water mass flow rate have the largest effect on the final size of the spray tower. Finally, a cross-current spray tower design was proposed for a Turbec T100 mGT because the sensitivity analysis showed that cross-current droplets injection meets the design constraints best.

Keywords: microturbine, micro Humid Air Turbine, saturation tower, spray tower, two-phase flow

NOMENCLATURE

Abbreviation

AHAT	Advanced Humid Air Turbine
CHAT	Cascaded Humidified Advanced Turbine
EvGT	Evaporative Gas Turbine
HAT	Humid Air Turbine
GT	Gas Turbine
mHAT	micro Humid Air Turbine
mGT	micro Gas Turbine
ODE	Ordinary Differential Equation
REVAP	REgenerative EVAPoration cycle
TIT	Turbine Inlet Temperature

Symbol

A	cross section [m²]
C	velocity [m/s]
D	diameter [m]
d	droplet diameter [m]
d_s	Sauter mean diameter [m]
F	force [N]
h	specific enthalpy [J/kg]
$\dot{m}$	mass flow rate [kg/s]
n	amount of droplets
p	pressure [Pa]
$\dot{Q}$	heat exchange rate [J/s]
T	temperature [K]
x	position along the axis of the saturator parallel to the direction of the compressed air [m]

Subscript

d	droplet
g	gas
i	component (film, droplets or gas core)
init	initial
l	loss
s	source
w	water

Superscript

'	per unit of length

1. INTRODUCTION

Gas Turbines (GTs) with mixed air/water as working fluid promise high electrical efficiency, high specific power output and low NO_x exhaust [1]. Among these mixed air/water GTs, the Humid Air Turbine (HAT), as initially proposed by Rao [2], has proven to have the highest potential [1]. Introducing an innovative component, the saturator, in the cycle layout will enhance the GT performance. However, only one pilot plant, the

Evaporative Gas Turbine (EvGT) project, has been constructed and tested in Lund since the development of the HAT cycle layout. The evaporative cycle without aftercooling achieved a thermal efficiency of approximately 35% [1, 3]. Later, different variants of the HAT were developed: the Cascaded Humidified Advanced Turbine (CHAT) [4] and the Advanced Humid Air Turbine (AHAT) [5, 6]. The CHAT cycle was developed to overcome the problem of the flow mismatch that exists between compressor and turbine in the original HAT design [4]. The AHAT cycle substitutes the intercooling from the HAT cycle by Water Atomizing inlet air Cooling (WAC) [6]. Hitachi built and tested a 4 MW-class AHAT pilot plant in Japan [7, 8]. Results of tests indicated a thermal efficiency of 40% of the power plant [7].

The effects of turning a micro Gas Turbine (mGT) into a micro Humid Air Turbine (mHAT) on the thermodynamic performance have been investigated by means of simulations [9-12]. Zhang et al. studied the effect of the humid air on the performance of the different mGT components [9]. Parente et al. determined the beneficial effect of adding water to the cycle on the global performance and studied the thermoeconomic efficiency of the mHAT, applied on current and future technologies [10, 11]. De Paepe et al. showed that the maximal potential for water injection in a mGT based HAT is 6 %wt of the compressor inlet air, which corresponds to a relative increase of thermal efficiency of 23% [12].

The saturator has been the subject of many studies performed by different researchers [13-20]. Lindquist et al. developed a physical model of the saturation tower and validated this model experimentally on the saturator constructed for the EvGT project in Lund [13]. Argen and Westermark investigated the possibility of a part-flow EvGT [14]. Parente et al. developed a code to simulate the evaporation in the saturator, using the hypothesis of a semi-ideal gas mixture [15]. Simulation results were validated against experimental results of the EvGT in Lund. Pedemonte et al. and Traverso investigated both experimentally the saturator performance on a specially designed test rig [17, 20]. Afterwards Pedemonte et al. used their results to develop empirical correlations to predict the humidification process in a pressurized saturator with packing [18]. Finally, Araki et al. designed, simulated and validated experimentally the saturator of the 4 MW AHAT power plant built in Japan [16, 19].

All of the previously discussed saturators or saturation towers use packing material to increase the contact area between the compressed air and the water, which will speed up the humidification process. Packing material however induces a pressure drop (approximate 400 Pa/m of packing [10]). Pressure losses in mGT have a large negative effect on mGT performance [21, 22]. For this reason, a new type of saturation tower has been developed using two-phase flow theory. Instead of increasing the contact area by using packing material, nozzles were used. The idea is that dividing the water in a large amount of small droplets will result in a large contact area between the liquid and the compressed air, which will provide the necessary surface for heat and mass transfer.

The final goal of this paper is to design the saturator for the mHAT version of the Turbec T100 mGT, installed in the labs of the Vrije Universiteit Brussel. During the design process, the main parameters of interest are saturator size and pressure drop. It is of great importance that both are lower than in a classical saturator with packing material. The secondary goal was to study the sensitivity of the humidification process to possible variations of the saturator inlet conditions. Eventually, a saturator will be constructed based upon the obtained recommendations.

In the first part of this paper, the modeling of the internal two-phase flow of the spray saturator is discussed. For every injection direction of the droplets, the considered assumptions are discussed. In the second part of this paper, the results of the different two-phase flow simulations for the different injection strategies are presented and discussed. Sensitivity analysis is performed to indicate the crucial parameters. In the final part of the paper, a conservative design for the saturator is proposed based on results of the sensitivity analysis.

2. MODELLING

In this section, first the mHAT cycle layout is discussed in order to situate the saturator in the cycle. Secondly, the used two-phase flow model is presented. The model is based on a model developed by Bram [23]. Rather than fully calculating the behaviour of the droplets by means of 3D computational fluid dynamics, a simplified 1D model is used to predict the optimal size of the saturator for full humidification of the hot compressed air.

2.1 mHAT cycle layout

The model of the mHAT cycle is based on the Turbec T100 mGT (see Figure 1). Air is compressed in the compressor (1). Rather than routing the compressed air directly to the recuperator, the air is humidified in the saturator, by means of an excess of water (2). The saturated air-water mixture is preheated by the exhaust gasses in the recuperator (3). Afterwards, the air-vapour mixture is heated till maximal Turbine Inlet Temperature (TIT) by burning natural gas in the combustor (4). Expansion over the turbine (5) provides the necessary power to drive the compressor and the high speed generator for electric power production (not included in Figure 1). After preheating the compressed saturated air, exhaust gasses are used to heat the excess water returning from the saturator. Feed water to replace the evaporated water is added to the water cycle (7). De Paepe et al. simulated the whole cycle, using a black box method. [12]. The working parameters of the saturator can be found in

Copyright © 2013 by ICAE2013

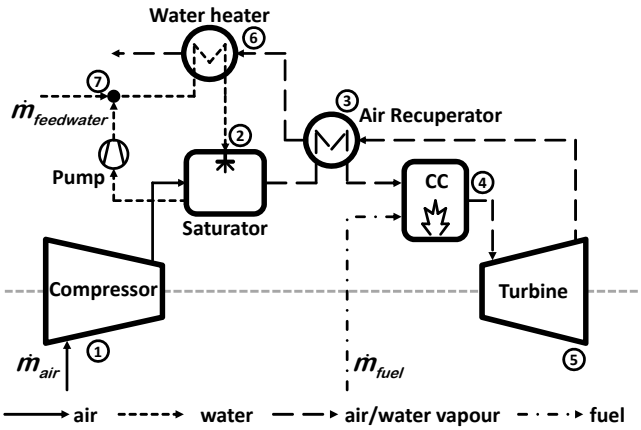

Figure 1: The mHAT, based on the original T100 mGT layout, involves next to the compressor (1), the combustion chamber (4) and a turbine (5), a saturator (2) to humidify the compressed air before preheating in the recuperator (3). The water heater (6) is used to provide the necessary hot water for the saturator. Evaporated water is replaced by feed water (7).

Table 1. The amount of evaporated water is rather low compared to the amount of injected water (2%). The large amount of water is however necessary to provide the necessary contact area for evaporation. This large amount of circulating water has an influence on the mHAT global performance. As indicated in [12], the loss in efficiency to the necessary pump power depends on the total amount of circulating water, but also on the used injection pressure. For a total injected amount of water of 2.5 kg/s at 0.5 bar pressure difference, losses are equal to 0.1% absolute efficiency decrease, which is low compared to the 7% absolute efficiency increase due to the water injection [12].

Table 1: Inlet conditions of the saturator.

	Air		Water	
	in	out	in	out
$\dot{m}\left[\mathrm{kg/s}\right]$	0.600	0.645	2.545	2.500
$T\left[^{\circ}\mathrm{C}\right]$	177	78	82	78
$p\left[\mathrm{bar}\right]$	3.7	$p_{\mathrm{air}}^{\mathrm{out}}$ (1)	$p_{\mathrm{w}}^{\mathrm{in}}$ (2)	$p_{\mathrm{w}}^{\mathrm{out}} = p_{\mathrm{air}}^{\mathrm{out}}$ (3)

(1) The pressure of the outgoing air depends on the total loss of pressure, which will be determined when designing the saturation tower.
(2) The pressure of the incoming water depends on the used nozzle to introduce the water.
(3) The pressure of the outgoing water is equal to the pressure of the outgoing air.

2.2 Two-phase flow model

To model the saturator, a previously developed method by Bram [23], the 1D Non-Adiabatic Annular Two-Phase Model has been modified. The model was constructed in the scope of the REgenerative EVAPoration (REVAP®) project [24]. The goal of this project was the development of a humidified turbine without saturator. The model distinguishes three different components in the flow:

- Gas core
- Liquid film
- Dispersed droplets

Each different component is seen in the model as a separated phase, which has a specific mass, momentum and energy. Different types of interaction exist between the different components of the flow (Figure 2).

In this case, the saturator is considered adiabatic and perfectly insulated from the environment, so the heat exchange with the surrounding can be neglected. In the case where nozzles are used to generate the droplets, there will be no uniform droplet diameter. Each different type of nozzle produces a specific distribution of droplets. A possible way to describe this is by using a discrete distribution of droplets with several representative diameters. All categories of droplet are thus seen as separated fractions, with own conservation equations. This would however make the model too complex. The final goal is to give a conservative design of the saturator and not to describe the exact internal behaviour of the droplets. Another possible solution is using the Sauter mean diameter (d_s) of the droplets. This diameter has the same ratio of surface to mass as the total droplet population. Mathematically:

$$d_s = \frac{\sum_{j=1}^{k} n_j d_j^3}{\sum_{j=1}^{k} n_j d_j^2}, \qquad (1)$$

where n_j is equal to the amount of droplets with diameter d_j and k is equal to the total number of droplets categories.

The next subsections present the models made to describe the three possible injection strategies: co-, counter- and cross current. In the co-current injection, the droplets are injected in the direction of the moving gas flow. In counter-current injection, the droplets are injected in the opposite direction of the moving gas core. In the

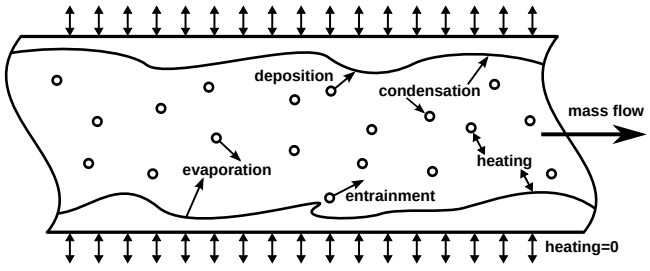

Figure 2: Annular dispersed 2-phase flow phenomena covering heat exchange and mass transfer between the different phases; through evaporation, condensation, entrainment and deposition of droplets.

Copyright © 2013 by ICAE2013

cross-flow, the droplets are injected perpendicular to the moving gas flow.

2.2.1 Co-current model

Mass conservation applies over each different section for each component, so one can write:

$$\frac{\mathrm{d}\dot{m}_i}{\mathrm{d}x} = \dot{m}_{\mathrm{s},i} - \dot{m}_{\mathrm{l},i}\,, \tag{2}$$

where i indicates the different component (gas, film or droplets). The source term $\dot{m}_{\mathrm{s},i}$ combines all possible sources to the specific phase. For the droplets, for example, this combines the amount of water condensation from the gas core back to the droplets together with the amount of entrained droplets in the considered section of the saturator. The loss term $\dot{m}_{\mathrm{l},i}$ combines all possible mass losses of the considered phase in the considered section. For the droplets, $\dot{m}_{\mathrm{l},i}$ is equal to the sum of the amount of water that evaporates from the droplets into the gas core and the amount of droplets that are deposited in the film.

Conservation of momentum gives

$$\frac{\mathrm{d}\left(\dot{m}_i C_i\right)}{\mathrm{d}x} + A_i \frac{\mathrm{d}p}{\mathrm{d}x} = F_i' + \dot{m}_{\mathrm{s},i} C_i - \dot{m}_{\mathrm{l},i} C_i\,, \tag{3}$$

where F_i' is the combined force, like friction between the different components, applied on the different components and A_i is the part of the cross section occupied by the component. Since only one dimension is considered, the effect of gravity is only taken into account when a vertical flow is considered. Results indicated that the fraction of gravity in the momentum change is generally smaller than 12% during the evaporation process.

Finally, the energy equations are

$$\frac{\mathrm{d}\left(\dot{m}_i h_i\right)}{\mathrm{d}x} = \dot{m}_{\mathrm{s},i} h_{\mathrm{s},i} - \dot{m}_{\mathrm{l},i} h_{\mathrm{l},i} + \dot{Q}_i' + F_i' C_i\,, \tag{4}$$

where $\dot{Q}'$ is the heat exchange between the different phases.

Equations (2), (3) and (4) result into a set of 9 Ordinary Differential Equations (ODEs) with 10 unknown parameters ($\dot{m}_i$, C_i , h_i and p). By differentiating the following equations, the system of ODEs can be closed [23]:

- the ideal gas law;
- the relations between mass flow rate and velocity;
- the sum of all flow sections A_i ;
- the change in molecular weight of the gas core;
- the enthalpy-temperature relation of the gas core;
- the evolution of the droplet mass.

In the case of co-current injection of the droplets, the ODEs can be solved directly, using a variable step size ODE-solver, ode15s, implemented in Matlab [25]. The stability of the solver was tested by Bram [23].

In the simulations, all different injection positions (see Figure 3) were investigated. This means that depending on the direction of movement of the gas and droplets, gravity is excluded (Figure 3(b)) from Eqs. (3) and (4) or included (Figure 3, (a) and (c)).

2.2.2 Counter-current model

The equations described in the previous section were also used for counter-current simulations. However the correlations for the different phenomena, like droplets entrainment and deposition were changed into the empirical correlations that can be applied for counter-current flow, since all phenomena are function of flow direction.

In the counter- and cross-current model, the film is neglected. The fraction of heat exchange and evaporation is very small compared to the droplets, since the contact area is some orders of magnitude smaller than the total droplets area. For typical values of inlet parameters, the mass transfer from the droplets to the gas is 10000 times bigger than the mass transfer from the film to the gas. In this case, the film is seen as a loss.

In the co-current model, inlet conditions of gas core, droplets and film were available at the same side of the saturator. In the counter current case, conditions of water phases are on a different side of the saturator than the gas core. This has some implication for solving the problem. Here the ODEs need to be solved in an iterative way. The major difficulty in this case is the tower length. In the co-current case, the set of ODEs can be solved over a long tower. Results of relative humidity will indicate the point of full humidification of the compressed air. This point indicates the minimal necessary saturator length. Making the saturator longer will have no effect on the outlet conditions of the stream. In the counter current case, a different length will result in a different final solution, meaning different outlet conditions. An additional difficulty is that not every combination of parameters will lead to a solution. The initial velocity of the droplets needs to be higher than in the co-current case, since the droplets have to travel against the air flow and are exposed to high friction forces. Especially the small droplets will encounter difficulties in reaching the bottom of the saturator and will most likely turn, which changes the counter-flow into a co-

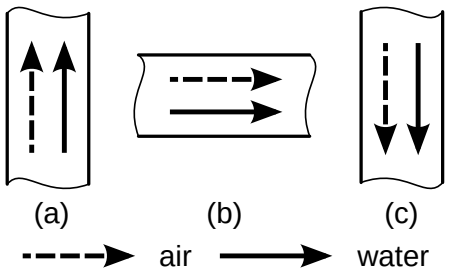

Figure 3: We evaluated these layouts of a co-current saturator: upwards (a), horizontal (b) and downwards (c) injection, to investigate the importance of gravity.

Copyright © 2013 by ICAE2013

current flow. Higher injection velocity requires however higher pressure difference over the nozzle.

The different considered injection schemes for simulations are summarized in Figure 4.

2.2.3 Cross-current model

For simulating the cross-current model, at least 2D-simulations are required, since the droplets will move in a direction perpendicular to the gas flow. However, by applying some conservative simplifications to the model, a 1D-model can be used to simulate cross-current:

- droplets are considered standing still from the point of view of the gas core;
- correct relative velocity (vector sum of droplet and gas velocity) is used to calculate the heat and mass transfer coefficients;
- the film is neglected and seen as a loss of water mass flow;
- the droplet temperature, as a conservative choice, is taken equal to the temperature of the outgoing water (78°C). Calculating the temperature profile of the droplets is not possible since 1D-simulations are preformed, so the temperature is kept constant along the droplet trajectory. Thermodynamic simulations of the saturator have shown that the water temperature does not change much (4°C: see Table 1);
- droplets are homogeneous distributed over the length and width of the saturator. The total amount of droplets per cross section depends on the height and the initial velocity. Based upon these parameters, the residence time can be calculated. Thus in the cross flow case, the tower length also needs to be predefined, as in the counter current model;
- droplet diameters are also considered constant along the droplet trajectory. Only 2% of the total water flow rate will evaporate (Table 1) along the full length of the tower. Since most mass transfer occurs in the first section of the tower (Figure 11(a)), the droplet diameter in this section will reduce the most (3%), which is still rather limited.

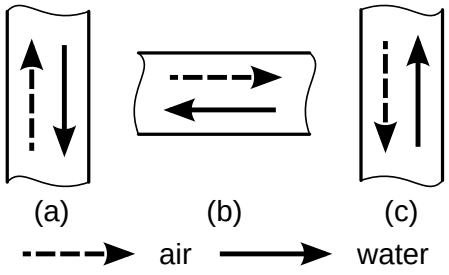

Figure 4: Evaluated layouts of a counter-current saturator, based on gas flow direction: upwards (a), horizontal gas flow (b) and downwards (c).

The possible cross-current injection schemes are indicated in Figure 5. Figure 6 shows the different droplet trajectories in the saturator, using the different injection schemes from Figure 5. Simulations are conducted using the same inlet conditions as used in cross-current saturator simulations (see 3.1.3) and neglecting the heat and mass transfer. The x-axis is defined parallel to the gas flow direction, while the y-axis is parallel to the injection direction. In case (b), where the gas is moving downward and droplets are injected horizontally, droplets do not reach the other side of the saturator, but are dragged along the tower, which results thus in a co-current flow. In this case, the hypothesis of droplets standing still is no longer valid. Case (b) was not considered in simulation. In case (d), droplets are just falling back down. This results in coalescence between the up going and the falling droplets, resulting in larger droplets and thus less contact area. In addition, there is no contact between the droplets and the compressed air in the upper section of the saturator. This will result in not fully saturated air. This case is thus also not considered in the simulations. Finally, for case (a) and (c), droplets will move along the cross section in the direction of the gas flow. The displacement of droplets is however limited (0.05m in case (a) and 0.13m in case (c)) and there is

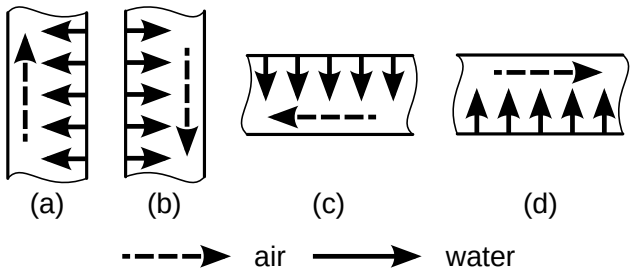

Figure 5: Possible injection schemes for a cross-current saturator, based on gas flow direction: upwards (a), downwards (b), horizontal - droplets injected downwards (c) and horizontal - droplets injected upwards (d).

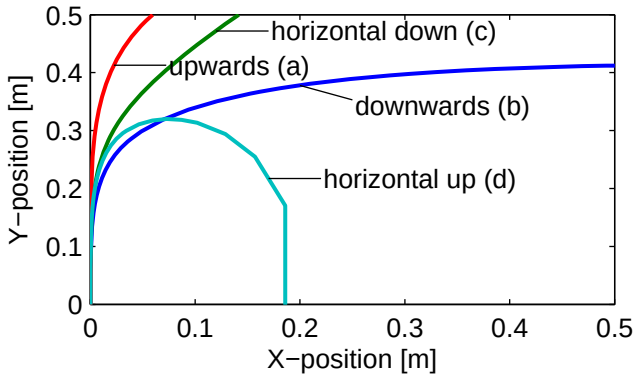

Figure 6: Droplet flow trajectory simulations indicating droplets move 0.13m in the x-direction for injection scheme (c) for a cross-current saturator.

Copyright © 2013 by ICAE2013

no droplet coalescence. All droplets follow the same trajectory, since the gas velocity does not change much as shown in Figure 11(c).

3. RESULTS

In the first section, the results of the different injection principles (co-, counter- and cross-current) are presented. In this section, the focus is on the evaporation process. Only the main thermodynamic parameters are discussed. In the second section, results of the sensitivity analysis are shown. The effects of the variation of different parameters on the humidification process and pressure drop are discussed.

3.1 Two-phase flow simulations

3.1.1 Co-current

Figure 7 shows the results of co-current flow simulations conducted using the inlet conditions as described in Table 1. Inlet conditions, using common nozzles and saturator size, are:

- $d_s = 0.1\,\mathrm{mm}$,
- $D = 0.5\,\mathrm{m}$,
- $C_\mathrm{d} = 20\,\mathrm{m/s}$.

In the co-current case, a cylindrical saturator is assumed, since the circular cross section matches best the nozzle spray cone. In this case, to exclude the effect of gravity on the performance, a horizontal saturator, with horizontal gas and droplet flow is assumed (case (b), Figure 3).

Most of the heat and mass transfer happens within the first part of the saturator, just after the injection point (Figure 7(a)). At this point, the driving force – low relative humidity (Figure 7(e)), thus low vapour pressure in the gas – is very high. The higher the relative humidity becomes, the more the mass transfer process is slowed down. Due to this high evaporation rate, droplet, film and gas temperature all decrease, because all energy is necessary to evaporate the water (Figure 7(b)). Final equilibrium temperature for droplets, film and gas is below their initial temperature. The droplets continuously slow down, due to the friction with the gas (Figure 7(c)). In the first section of the saturator, the gas will speed up due to the friction with the droplets and the evaporation (increasing gas volume). After the entrance region, the friction with the wall and film starts to become more important, resulting in a decreasing gas velocity. Film velocity remains almost constant and very low. Droplet diameter only varies little during the evaporation process (Figure 7(d)). The small droplet diameter variation (max. 0.6%) is a result of the large amount of injected water. Only 2% or 0.45 kg of the total amount of injected water will evaporate. After 0.15m, the compressed air reaches full saturation (100% relative humidity, see Figure 7(e)). Once this point is reached, the gas mass flow remains constant, but the droplet mass flow rate is continuously decreasing, due to the deposition of droplets in the film. Finally pressure increases during the evaporation process, as indicated on Figure 7(f). The behaviour of the pressure is rather complex and needs some additional study. For this reason, the saturator has been elongated (5m total length) to better show the effect of water injection on the pressure.

Pressure simulations show the effect of the droplets injection and the evaporation process on velocity and pressure (Figure 8). In the inlet region, pressure is increasing. The pressure is a complex parameter, whose behaviour is influenced by several effects that counteract. On the one hand, pressure will increase due to the evaporation of the water. On the other hand, pressure will decrease due to the friction between the gas core and the wall (or film) and the lower temperature. Finally, there is also the effect of the presence of the droplets. In case $C_{\mathrm{d,init}} > C_{\mathrm{g,init}}$, pressure will increase in the entrance region (Figure 8), in the case where $C_{\mathrm{d,init}} < C_{\mathrm{g,init}}$, pressure will decrease (Figure 9). Finally, after the pressure has reached a maximum, it starts to decrease. In this phase, droplets, film and gas are in thermal equilibrium (same temperature and relative humidity of 100%, so that there is no more heat and mass transfer). There is no more friction between the droplets and the gas core since $C_\mathrm{d} = C_\mathrm{g}$. The only remaining effect is the friction between the gas core and the film/wall, which will decrease the pressure. Since the velocity difference between gas core and film is low, pressure losses are limited in this region.

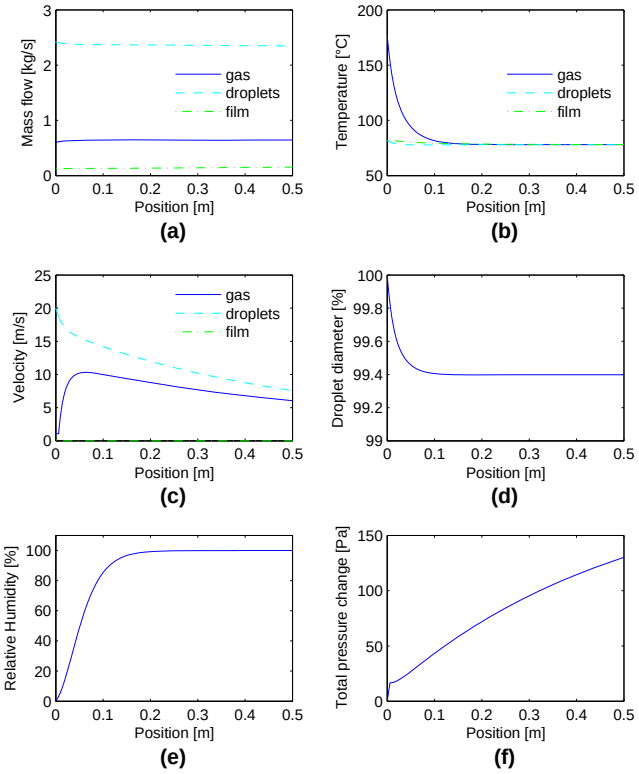

Figure 7: Simulation results of a co-current saturator, indicating necessary tower length for fully saturated air is 0.15m.

Copyright © 2013 by ICAE2013

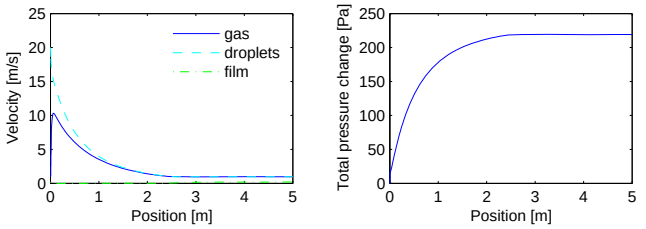

Figure 8: Velocity and pressure results in extended (5m) saturator where initial droplet velocity is larger than the initial gas velocity.

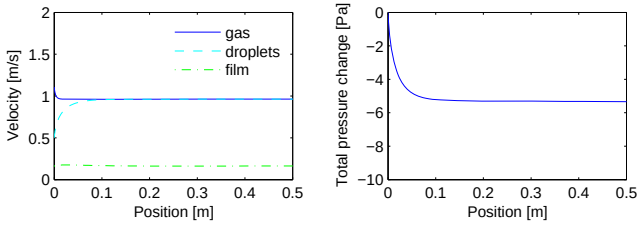

Figure 9: Velocity and pressure results in saturator where initial droplet velocity is smaller than the initial gas velocity.

3.1.2 Counter-current

The results of the counter-current flow simulations, using inlet conditions from Table 1, are shown in Figure 10. Further inlet conditions are:

- $d_s = 0.5\ \text{mm}$,
- $D = 0.5\text{m}$,
- $length = 0.5\text{m}$,
- $C_\text{d} = 8\ \text{m/s}$.

Finally, injection scheme (a) from Figure 4 is used to generate the results of Figure 10.

The mass and heat transfer occurs in the gas entrance section (Figure 10(a)), due to the large driving force (low relative humidity and big temperature difference, Figure 10(b) and (d)). The temperature of the outgoing saturated compressed air is 82°C. Both gas and droplet velocity decrease continuous due to friction (Figure 10(c)). Droplet diameter reduces 0.8% along the saturator axis (Figure 10(d)). This is more than in the co-current case (0.6%), but since the outgoing air temperature is higher, more water is evaporated to reach 100% relative humidity after 0.5m (Figure 10(e)). Pressure loss is larger than in the co-current case, since the gas and droplets are moving in the opposite direction, resulting in larger friction forces (Figure 10(f)).

3.1.3 Cross-current

The results of the cross-current flow simulations are shown in Figure 11. The inlet conditions as described in Table 1 are used, except for the droplet temperature. As mentioned before, the droplet temperature is kept constant and equal to the outlet temperature ($T_\text{d} = 78°\text{C}$). For these simulations, injection scheme (c) from Figure 5 is used. Further inlet conditions are:

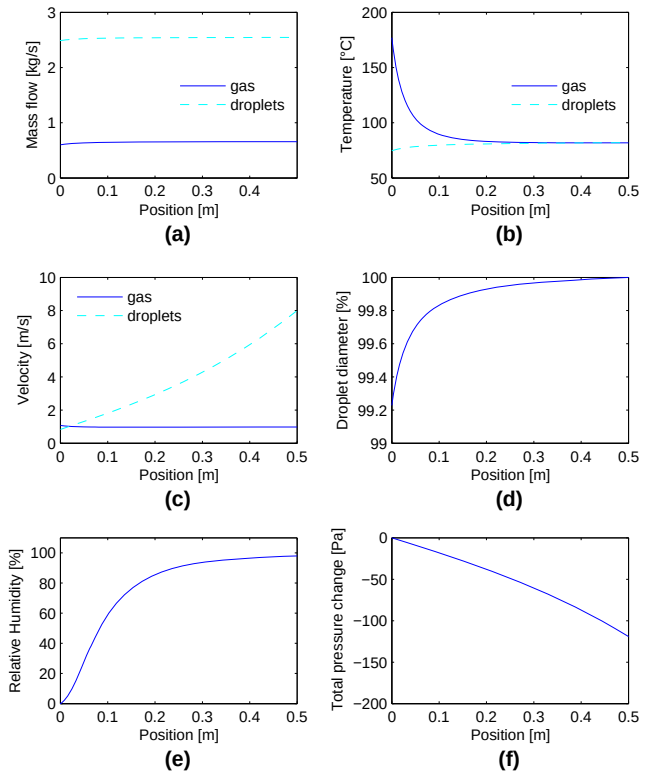

Figure 10: Simulation results of a counter-current saturator, indicating necessary tower length for fully saturated air is 0.5m.

- $d_s = 0.5\ \text{mm}$,
- $height = 0.5\text{m}$,
- $width = 0.3\text{m}$,
- $lenght = 0.5\text{m}$,
- $C_\text{d} = 20\ \text{m/s}$.

In the cross-current flow, a rectangular cross section has been used, for the ease of simulations. The final cross section design will depend on the spray cone of the nozzle. The cross section should match the spray cone, in order to obtain an optimal contact between the air flow and injected droplets.

Since the droplet temperature is kept constant and droplets move in a direction perpendicular to the gas flow, droplet temperature, mass flow and velocity are not shown on Figure 11.

Results of simulation clearly show in Figure 11(a) that the mass transfer occurs again in the first part of the saturator, due to the large driving force (low relative humidity). The compressed air cools down, till the equilibrium temperature of 78°C is reached (Figure 11(b)). According to Figure 11(a), saturation is already reached after 0.13m. Shortening the tower is however not possible. If the tower length is changed, the amount of injected water also needs to be changed, since we assume a homogeneous distribution of the droplets. Changing this amount however, will affect the performance of the water heater of the mHAT, and will

Copyright © 2013 by ICAE2013

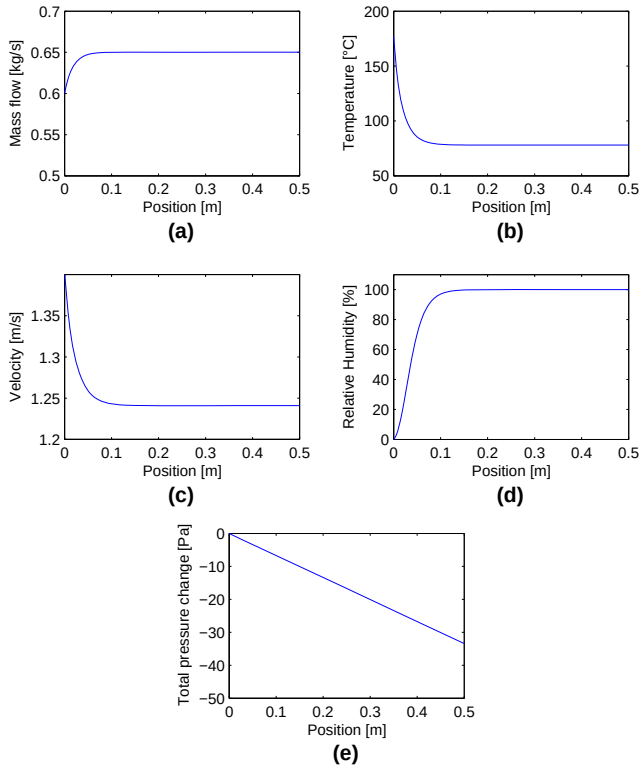

Figure 11: Simulation results of a cross-current saturator, indicating necessary tower length for fully saturated air is 0.5m.

results in a lower mHAT performance. The gas is also slowed down by the friction between the gas core and wall and droplets, since the droplets are moving perpendicular to the gas flow (Figure 11(c)). Final saturation is reached after 0.15m, as indicated on Figure 11(d). Pressure simulations indicate that the pressure decreases over the length of the saturation tower due to the friction with the wall and the droplet (Figure 11(e)). Total pressure losses are however very low (less than 40 Pa or 0.01% of the total pressure).

3.2 Sensitivity analysis

For the sensitivity analysis, all different input variables have been varied over a specific range. The range was chosen based on the possible physical variations of the parameters. The main goal of the sensitivity analysis was to determine the effect of each parameter on the minimal length of the saturator and on the total pressure change.

One can divide the parameters into two main groups: the design parameters and the thermodynamic parameters. The design parameters, d_s , A , $\dot{m}_w$, T_w and C_d , can be chosen in order to minimize the size of the saturator and to minimize the pressure drop. In the sensitivity analysis, these parameters are varied in order to gain insight in the effect of these parameters on the saturator length. The thermodynamic properties of the compressed air are controlled by the mGT control system. The control of these parameters is not within reach of the designer of the saturator; however variation of these parameters is likely. Depending on the inlet air conditions and the operator chosen set points (produced electrical power), the mGT control system will change the rotation speed of the compressor, which will of course have an effect on compressor outlet condition and thus on the saturator inlet conditions (T_g , p and $\dot{m}_g$) as well. The saturator needs to fully saturate the compressed air in all cases, so not only in the case where the saturator inlet conditions are as in Table 1. In case there is a small variation on these parameters, compressed air leaving the saturation tower still needs to be saturated. In the sensitivity analysis, these parameters are thus varied over their operational range, to verify if the compressed air is fully humidified when leaving the saturator.

Major parameters of interest are the relative humidity and the pressure losses. The relative humidity needs to be 100% at the end of the saturator. Since the final goal is to design a saturator for the mHAT, an additional parameter of interest is the necessary length of the tower to achieve the 100% relative humidity (saturation length). Results of parameter variation on relative humidity and pressure change for the different injection strategies – co-, counter- and cross-current injection – are presented in following subsections.

3.2.1 Co-current

Figure 12 shows the results of the sensitivity analysis on the relative humidity. Film flow has been neglected to save calculation time. For the sensitivity analysis of the co-current model, the inlet conditions of Table 1 are used in combination with the geometric conditions given in section 3.1.1. Every time, the indicated parameter is varied over the specified range while all other parameters were kept constant to really focus on the influence of the considered parameter.

Droplet diameter has a huge impact on saturation length (see Figure 12). The droplet diameter determines the contact area for heat exchange and mass transfer. A droplet diameter twice as large results in a reduction of contact area by 4. This has a severe negative effect on heat and mass transfer, since these are two effects that appear on the contact surface of both phases. Both droplet velocity and cross section size (here in the form of the saturator diameter) have a rather small influence on the saturation length (Figure 12). The cross section determines the gas velocity. A large velocity difference between gas and droplet has a positive effect on heat and mass transfer. On the other hand, this effect is not strong enough to compensate the faster moving gas core, which results in a longer saturation length. Figure 12 also shows that water mass flow rate has a positive effect on the saturation length, since more water will result in more droplets and thus more contact area. The influence of the air and water

Copyright © 2013 by ICAE2013

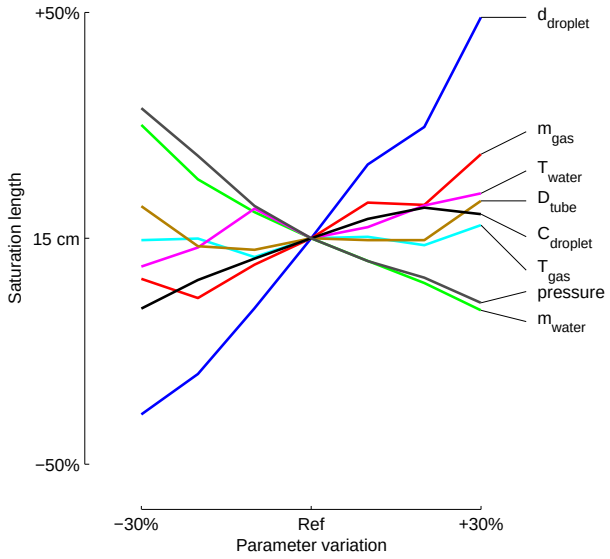

Figure 12: Results of variation of the parameters show that droplet diameter and water mass flow rate are the most crucial parameters for humidification length in co-current injection.

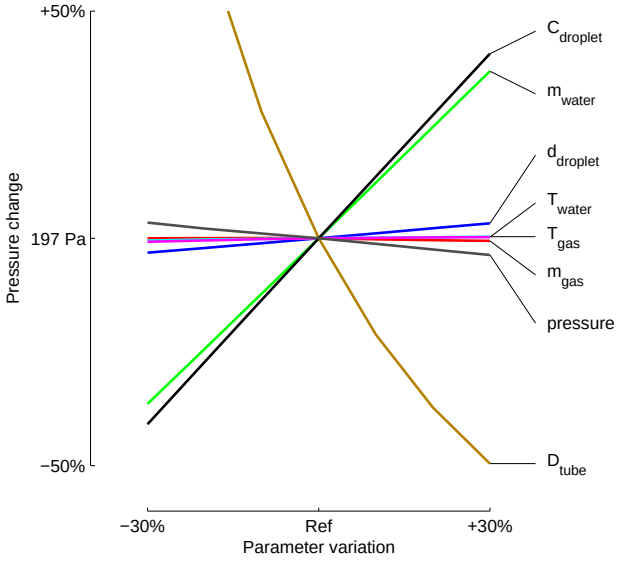

Figure 13: Results of variation of the parameters show that water mass flow rate and saturator diameter have the largest effect on total pressure change in co-current injection.

temperature on the saturator length is low (Figure 12). A higher temperature has a positive effect on the heat and mass transfer, which should speed up the evaporation process. However it requires more water evaporation to achieve a 100% relative humidity. So even though the evaporation process is enhanced, saturation length remains more or less constant since more water needs to evaporate to achieve the saturation condition. The mass flow of the gas has only a minor effect on the saturation length. A lower mass flow results in a lower amount of water that needs to be evaporated for saturation. Figure 12 shows that the gas pressure has a large effect on the saturation length, however variations of 30% on the total pressure are rather large. Finally, simulations showed that the orientation of the saturator has no effect at all on the saturation length.

Figure 13 shows the effects of parameter variation on the pressure. In general, the parameters that influence the gas or droplet velocity and the total contact area, will influence the pressure change. Smaller droplets result in more contact surface, so more friction, which explains the increasing pressure at small droplet diameters (Figure 13). The droplet velocity has a major effect on pressure changes, as indicated on Figure 13. The higher the difference between droplet and gas velocity, the more pressure will increase, due to higher friction forces between both. Saturator diameter has the largest effect on pressure change, since it affects the gas velocity (Figure 13). A higher gas velocity results in higher pressure increase due to the interaction with the droplets in the entrance zone. When applying a longer saturator, the friction losses due to the higher gas velocity will be higher. The water mass flow rate has a major impact on pressure change (Figure 13). The larger the injected amount of water is, the more droplets there are. All these droplets are slowed down by the gas, which will increase the pressure. The more droplets that are injected, the higher the pressure increase will be. Figure 13 shows that both gas and water temperature have no effect on the pressure change. The gas mass flow rate has also no effect on pressure loss, since the gas velocity is rather low (1 m/s). Figure 13 showed that a different saturator inlet pressure has only a minor effect on pressure changes. Finally, the orientation of the tower has no effect on the pressure in the entrance region, but after this region, the effect of gravity is visible on the pressure change, however rather small (300 Pa for case (a) from Figure 3, 250 Pa for case (b) and finally 200 Pa for case (c)).

3.2.2 Counter-current

Figure 14 shows the results of the sensitivity analysis of counter-current water injection in the compressed air on the humidification length. For the sensitivity analysis of the counter-current model, the same inlet and boundary conditions as in Table 1 and section 3.1.2 are used.

Figure 14 clearly shows that the counter-current water injection is more sensitive to variation. For some variations of several parameters, no saturation was reached within the tower length or even droplets did not reached the end of the tower, resulting in no depicted results. This clearly highlights the narrow margin for counter-current droplet injection.

The droplet diameter, velocity, water mass flow and tower length have the largest effect on the humidification process (Figure 14). If the droplets are too large, saturation is not reached inside the saturator. But on the other hand,

Copyright © 2013 by ICAE2013

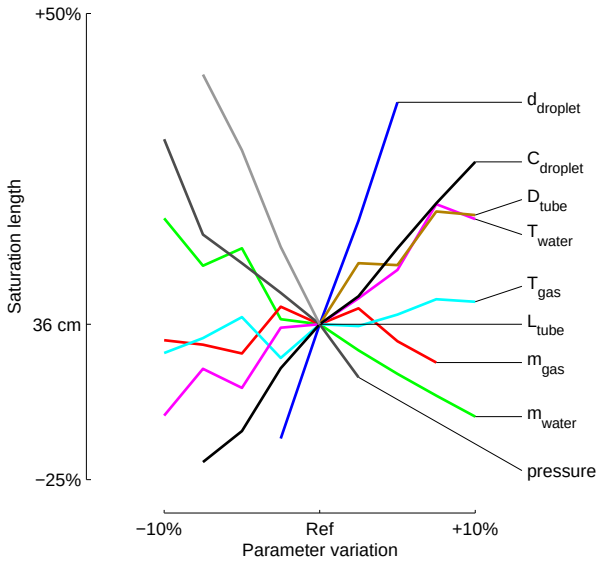

Figure 14: Results of variation of the parameters in counter-current injection, showing that droplet diameter, velocity, water mass flow and tower length are the most crucial parameters for humidification length.

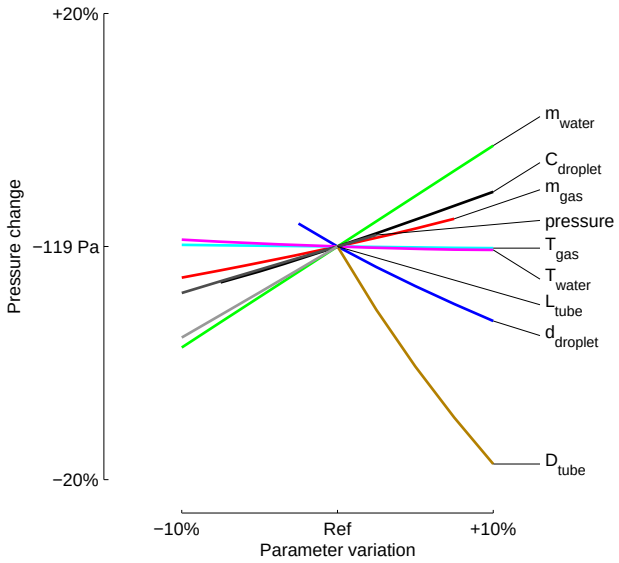

Figure 15: Results of variation of the design parameters in counter-current injection show that droplet velocity, water mass flow rate and tower width have the largest effect on total pressure change.

too small droplets with a low velocity, will not reach the end of the tower, due to friction with the gas. In this case, droplets are stopped, will coalesce and fall down, depending on the orientation of the tower. The higher the velocity, the faster the droplets will move through the saturator. So the compressed air has no time to saturate. With a too low velocity, however, it is possible that the droplets will not reach the saturator exhaust. The tube diameter has the same effect as the droplet velocity (see Figure 14), since the saturator diameter will change the gas velocity. A too large section will make the droplets pass too fast, while a too small section results in too high gas velocity and coupled friction, which augments the risk for droplet stagnation. The water mass flow rate determines the contact area between gas and water and it has a direct effect on saturation length. The tower length is also of great importance, as shown in Figure 14. If the tower is too short, the residence time of the droplets is not long enough to saturate the air. A too long tower however increases the risk of droplet stagnation. The effect of water and gas temperature and gas mass flow rate is limited. Finally, orientation has a minor effect on the saturation process.

Figure 15 shows the total pressure change results of the sensitivity analysis. All parameters that influence the contact area (like droplet diameter and water mass flow rate and the velocity difference between gas and water phase (Droplet velocity, saturator diameter and tower orientation), have a large influence on pressure drop, since the pressure drop is a function of these two parameters. Finally, in the counter-current injection case, the gas temperature and mass flow rate have little influence on the saturation process.

3.2.3 Cross-current

Figure 16 shows the results of the sensitivity analysis of cross-current water injection in the saturator. In the cross-current case, conditions of Table 1 and section 3.1.3 have been used.

A larger droplet diameter results in less contact area. If the droplets are too big, the compressed air will never reach saturation (Figure 16). Making the tower longer as in the co-current case is no option. The droplet velocity has a large effect on saturation length (Figure 16). The velocity will determine the residence time of the droplets in the saturator and thus the available droplets in the saturator. Changing the tower width has almost no effect on the saturation length, as indicated in Figure 16. Changing the tower width will only influence the gas velocity. Since the gas velocity is rather low (approximate 1 m/s), gas velocity does not change much with increasing width. The heat and mass transfer coefficient will thus vary little, resulting in no visible effect on the saturation length. The height of the saturator is on the other hand of great importance in the cross-current injection (Figure 16). The higher the saturator, the faster the 100% relative humidity is reached. A higher saturator contains more water than a lower, since the residence time of the droplets is longer. This provides a larger surface for heat exchange. Water mass flow rate has a large effect on saturation length, as indicated by Figure 16. The higher the water mass flow rate is, the more droplets there are, so the more contact area. The length of the tower has a minor effect on the saturation length. The droplets are distributed homogeneously along the longitudinal axis of the saturator. Making the saturator

Copyright © 2013 by ICAE2013

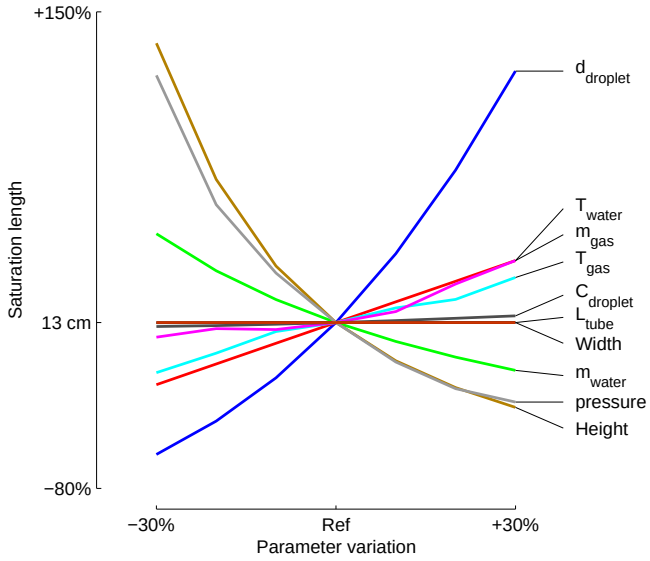

Figure 16: Results of variation of the parameters showing droplet diameter, tower height and water mass flow rate are the most crucial parameters for humidification length in cross-current injection.

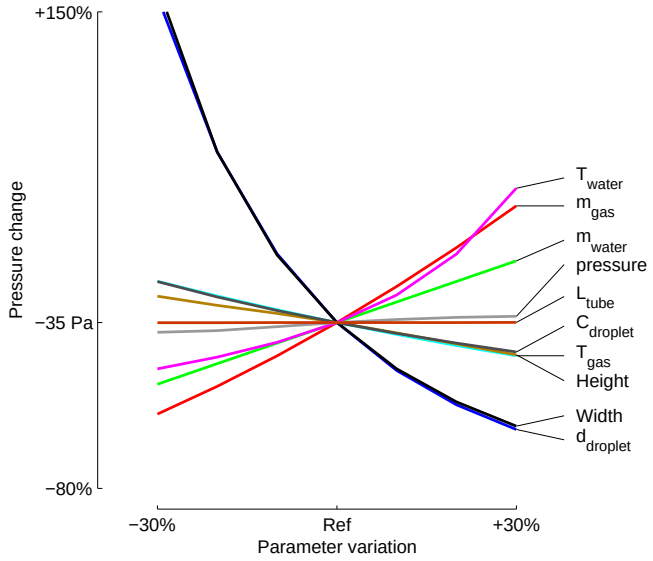

Figure 17: Results of variation of the design parameters in cross-current injection show that droplet diameter, cross section and tower length and width are the most crucial parameters for total pressure change.

longer results in a lower droplet density per cross section and thus a lower contact area per cross section, which explains the longer saturation length. Relative saturation length – saturation length normalized by the total tower length – remains the same. Saturation can only be reached by heightening the saturator. As in the co- and counter current case, both gas and water temperature have a minor effect on the saturation length (Figure 16). The gas mass flow rate has, as in the co-current case, a small effect on the saturation length. Finally Figure 16 shows that changing the pressure has only a minor effect on the saturation length. Using injection scheme (a) from Figure 5 results in a shorter saturation length (0.09m), since in this case; the movement of the droplets through the gas core is not influence by gravity, resulting in a longer residence time than in injection type (c) from Figure 5 (0.13m).

Simulations of the pressure drop in the cross-current injection show that in general the pressure drop is limited (Figure 17). A small droplet diameter provides a large contact area between both the gas and the droplets (Figure 17). This is positive for the heat exchange and mass transfer, but has however a negative effect on the pressure loss. The droplet velocity will determine the amount of droplets present in the saturator, as indicated by Figure 17. The lower the velocity, the larger the residence time of the droplets will be. A larger amount of droplets results in more friction. Width and height of the saturator determine the gas velocity. The higher the velocity, the higher the pressure loss will be (Figure 17). A higher water mass flow rate results in more droplets and higher friction forces with the gas, as can be seen in Figure 17. Figure 17 also shows that the tower length has no influence on the pressure drop. Gas and water temperature have a minor effect. Higher gas and water temperatures result in more evaporation, which has an effect on the gas velocity. In addition, the gas temperature will influence the density, which has also an effect on the velocity. Increasing the gas mass flow rate will increase the gas velocity and thus the friction. Finally, gas pressure has no effect on pressure changes as indicated in Figure 16. Orientation has a small influence on the pressure loss (less than 4 Pa).

3.3 Pressure drop

One of the main reasons for using a spray tower without packing material as saturator instead of a more traditional packed saturator was the lower pressure drop. By using spray injection, it is possible to reduce the pressure drop, since no packing material is used. In their simulations for the design of a packed saturator, Parente et al. [10] assumed a pressure drop of 400 Pa/m of packing height. Final simulations of a mHAT cycle, based upon a 100 kW_e mGT indicated a total packing volume of 0.08 m^3 is necessary to fully saturate the compressed air.

Out of these simulations, using empirical correlation to estimate pressure drop over cooling tower fills [26], total expected pressure drop over the packing could be calculated. This pressure drop is in the order of magnitude of 100 Pa, which corresponds to Parente's assumption [10].

Simulations of co- and cross-current injection of droplets have shown that the pressure drop is very limited. By carefully choosing the dimensions of the saturator, the nozzle (which will determine droplet velocity and diameter) and the amount of circulating water, the pressure loss can

Copyright © 2013 by ICAE2013

be limited. Simulations also showed that for the counter-current injection strategy, pressure drop is generally higher.

3.4 Saturator design

The final goal of the paper was to design a saturator that could be applied on the T100 mGT. The two major design parameters were pressure drop and size. The discussion on the pressure drop in the previous section has shown that it is possible to design a spray saturator with lower pressure losses than a traditional saturator. The second condition was the size of the saturator. Parente et al. [10] calculated that for a 100 kW_e mGT, a saturator with 0.08 m³ of packing is necessary to fully saturate the compressed air.

Simulations have shown that for both the co- and cross current case, using the dimensions as mentioned in sections 3.1.1 and 3.1.3, fully saturated air is reached after 0.25m and 0.13m. In the co-current case, droplets of 0.1 mm were used, while in the cross-current case, droplets of 0.5 mm could be used. In order to get smaller droplets, the injection pressure of the water over the nozzles needs to be higher. Sauter mean diameter of a nozzle at a specific pressure can only be determined experimentally. Each different nozzle has its own specification. For a standard industrial nozzles (Nozzle type: CAY2970 [27]), to reduce the droplet diameter by a factor 2, the pressure needs to be increased by a factor 2 (according measurements of the manufacturer) and thus a higher power loss to the auxiliaries. This would imply that in the co-current case, more power would be lost to the auxiliaries. In the co-current case, the higher saturator exhaust pressure results in a relative efficiency increase of 0.05%, compared to the 0.003% loss in the cross-current case. However the smaller necessary droplet diameter is penalized by a relative efficiency loss of 1.5% compared to the 0.15% loss in the cross-current case due to the higher necessary auxiliary power. Per extra 100W auxiliary power, electric efficiency is reduced by 0.1% relative [12]. However co-current injection has a positive effect on pressure loss, the loss through the auxiliaries to provide the smaller droplet diameter is of greater importance. Therefore, co-current injection of the droplets was decided not be been used.

Comparing simulations of counter- (Figure 10) and cross-current (Figure 11) flow shows that in both cases saturation can be reached in a 0.5m saturator. Sensitivity analysis results of counter-current flow however showed that saturation can only be reached in a small window of boundary conditions variation. For example in case the velocity is to low, droplets will turn around, in case velocity is too high, no saturation is reached. In the cross-current flow simulations, the final saturation length is less sensitive to variations of these inlet conditions. Since it was the goal to propose a conservative design for a saturation tower, it was decided to use cross-current injection, because sensitivity analysis results showed that cross-current injection is rather insensitive for possible parameter variations, while the operational window of the counter-current saturator is rather narrow. In addition, pressure loss is higher for the counter-current water injection.

So final design proposition would be a cross-current saturator, with following dimensions:

- $height = 0.5\text{m}$,
- $width = 0.3\text{m}$,
- $lenght = 0.5\text{m}$.

For the ease of implementation, horizontal gas flow (Figure 5, case (c)) will be used, since according to sensitivity analysis, there is little difference between case (a) and (c). The evacuation of the remaining water is easier. In case (a), the water will first move downward through the saturator wall, before it can be removed.

Total pressure loss over the saturator is equal to 33 Pa, which is better than a packed saturator (three times smaller) and reduces the efficiency loss by 0.005% absolute or 0.02% relative. The total size is equal to 0.075 m³, which is in the same order as the packed saturator proposed by Parente et al. [10].

4. CONCLUSION

A recuperated mGT can be transformed into a mHAT by introducing a novel component into the cycle, the saturator. This component will humidify the compressed air. Traditional saturators use packing material to increase the contact area between compressed air and water to enhance the heat and mass transfer between both. This packing material however introduces a pressure drop in the cycle, which has a negative effect on the global mHAT performance (0.01% efficiency loss per 100 Pa pressure drop). An alternative route for humidification is the spray tower. In this spray tower, water is injected as fine droplets. These droplets will provide the necessary surface for heat exchange.

For this paper, a two-phase flow model is developed for designing such a spray tower. The two major boundary conditions were pressure drop and saturator volume. The aim of this study was to develop a saturator with better performance than the classical saturator with packing. The two-phase flow model is also used to perform a sensitivity analysis to identify the parameter which variation will have the largest influence on global performance.

Simulation resulted in following results:

- Co-, counter- and cross-current 2-phase flow calculations for a saturator have been performed.
- It is possible to fully humidify the compressed air within a reasonable distance.
- Sensitivity analysis indicated droplet diameter and water flow rate as the most crucial parameters for all different flow configurations. Halving the droplet diameter results in twice the required auxiliary pump power, while doubling the water mass flow rate, also

Copyright © 2013 by ICAE2013

results in twice the required auxiliary power. Per 100W required auxiliary power, electric efficiency is reduced by 0.1%.

- Pressure drop was below the pressure drop of the classic saturator with packing material. Pressure drop is three times smaller, resulting in 0.02% less efficiency loss.

Based upon these results, a suggestion for saturator design has been made.

ACKNOWLEDGEMENT

The research was funded by the National Fund for Scientific Research (FWO).

REFERENCE

[1] Jonsson M, Yan J. Humidified gas turbines – a review of proposed and implemented cycles. Energy. 2005;30:1013-78.
[2] Rao AD. Process for producing power. US patent no. 4829763, 1989.
[3] Årgen ND, Westermark MO, Bartlett MA, Lindquist T. First Experiments on an Evaporative Gas Turbine Pilot Power Plant: Water Circuit Chemistry and Humidification Evaluation. Journal of Engineering for Gas Turbines and Power. 2002;124:96-102.
[4] Nakhamkin M, Swensen EC, Wilson JM, Gaul G, Polsky M. The Cascaded Humidified Advanced Turbine (CHAT). Journal of Engineering for Gas Turbines and Power. 1996;118:565-71.
[5] Higuchi S, Hatamiya S, Araki H, Marushima S. A Study of Performance on Advanced Humid Air Turbine Systems. Journal of the Gas Turbine Society of Japan. 2006;34:54-61.
[6] Dodo S, Nakano S, Inoue T, Ichinose M, Yagi M, Tsubouchi K, et al. Development of an Advanced Microturbine System Using Humid Air Turbine Cycle. ASME Conference Proceedings. 2004;2004:167-74.
[7] Higuchi S, Koganezawa T, Horiuchi Y, Araki H, Shibata T, Marushima S. Test Results From the Advanced Humid Air Turbine System Pilot Plant: Part 1 – Overall Performance. ASME Conference Proceedings. 2008;2008:691-700.
[8] Araki H, Koganezawa T, Myouren C, Higuchi S, Takahashi T, Eta T. Experimental and Analytical Study on the Operation Characteristics of the AHAT System. Journal of Engineering for Gas Turbines and Power. 2012;134:051701 (8 pages)
[9] Zhang S, Xiao Y. Steady-State Off-Design Thermodynamic Performance Analysis of a Humid Air Turbine Based on a Micro Turbine. ASME Conference Proceedings. 2006;2006:287-96.
[10] Parente J, Traverso A, Massardo AF. Micro Humid Air Cycle: Part A – Thermodynamic and Technical Aspects. ASME Conference Proceedings. 2003;2003:221-9.
[11] Parente J, Traverso A, Massardo AF. Micro Humid Air Cycle: Part B – Thermoeconomic Analysis. ASME Conference Proceedings. 2003;2003:231-9.
[12] De Paepe W, Delattin F, Bram S, De ruyck J. Water injection in a micro gas turbine – Assessment of the performance using a black box method. Applied Energy. 2012; :http://dx.doi.org/10.1016/j.apenergy.2012.11.006.
[13] Lindquist T, Thern M, Torisson T. Experimental and Theoretical Results of a Humidification Tower in an Evaporative Gas Turbine Cycle Pilot Plant. ASME Conference Proceedings. 2002;2002:475-84.
[14] Årgen ND, Westermark MOJ. Design Study of Part-Flow Evaporative Gas Turbine Cycles: Performance and Equipment Sizing – Part I: Aeroderivative Core. Journal of Engineering for Gas Turbines and Power. 2003;125:201-15.
[15] Parente JOS, Traverso A, Massardo AF. Saturator analysis for an evaporative gas turbine cycle. Applied Thermal Engineering. 2003;23:1275 - 93.
[16] Araki H, Higuchi S, Marushima S, Hatamiya S. Design Study of a Humidification Tower for the Advanced Humid Air Turbine System. Journal of Engineering for Gas Turbines and Power. 2006;128:543-50.
[17] Pedemonte AA, Traverso A, Massardo AF. Experimental analysis of pressurised humidification tower for humid air gas turbine cycles. Part A: Experimental campaign. Applied Thermal Engineering. 2008;28:1711 - 25.
[18] Pedemonte AA, Traverso A, Massardo AF. Experimental analysis of pressurised humidification tower for humid air gas turbine cycles. Part B: Correlation of experimental data. Applied Thermal Engineering. 2008;28:1623 - 9.
[19] Araki H, Higuchi S, Koganezawa T, Marushima S, Hatamiya S, Tsukamoto M. Test Results From the Advanced Humid Air Turbine System Pilot Plant: Part 2 – Humidification, Water Recovery and Water Quality. ASME Conference Proceedings. 2008;2008:701-12.
[20] Traverso A. Humidification tower for humid air gas turbine cycles: Experimental analysis. Energy. 2010;35:894 - 901.
[21] Lagerstrom G, Xie M. High Performance and Cost Effective Recuperator for Micro-Gas Turbines. ASME Conference Proceedings. 2002;2002:1003-7.
[22] Zanger J, Widenhorn A, Aigner M. Experimental Investigations of Pressure Losses on the Performance of a Micro Gas Turbine System. Journal of Engineering for Gas Turbines and Power. 2011;133:082302 (9 pages)
[23] Bram S. The thermodynamic Potential of evaporative regeneration in gas turbine cycles for power production. Pleinlaan 2, 1050 Brussels, Belgium: Vrije Universiteit Brussel; 2002.
[24] De Ruyck J, Bram S, Allard G. REVAP® Cycle: A New Evaporative Cycle Without Saturation Tower. Journal of Engineering for Gas Turbines and Power. 1997;119:893-7.
[25] Mathworks. Matlab R2012a. Retrieved from *www.mathworks.com* Accessed: December 2012.
[26] Kloppers JC, Kröger DG. Loss coefficient correlation for wet-cooling tower fills. Applied Thermal Engineering. 2003;23:2201-11.
[27] PNR Benelux Inc. Groot-Bijgaarden, Belgium. Retrieved from *http://www.pnr.be/* Accessed: December 2012.

Copyright © 2013 by ICAE2013